Magyarhoni Földtani Társulat
Földtani Közlöny
Hungarian Geological Society

155/4, 291–302., Budapest, 2025

DOI: 10.23928/foldt.kozl.2025.155.4.291

Mineralogical mosaics from the Carpathian–Pannonian region 6

FEHÉR, Béla[1]*, SZAKÁLL, Sándor[2], LÁZÁR, Károly[3], ZAJZON, Norbert[2], BULÁTKÓ-DEBUS, Délia[2], KRISTÁLY, Ferenc[2]

[1]Department of Mineralogy, Herman Ottó Museum, Kossuth utca 13., H-3525 Miskolc, Hungary
[2]Institute of Exploration Geosciences, University of Miskolc, H-3515 Miskolc-Egyetemváros, Hungary
[3]HUN-REN Centre for Energy Research, Konkoly-Thege Miklós út 29–33., H-1121 Budapest, Hungary
*E-mail: feherbela@t-online.hu

Ásványtani mozaikok a Kárpát-Pannon régióból 6.

Összefoglalás

Hatodik tanulmányunkban további információkat közlünk a Kárpát–Pannon régió új ásványtani eredményeiből. Az adatokat országok és lelőhelyek szerint csoportosítottuk. Az egyes „mozaikdarabokban" az ásványok pontos leírására és – döntően XRPD, SEM-EDX és EMPA általi – meghatározására, illetve a paragenezis tömör bemutatására koncentráltunk. A tanulmányunkban szereplő ásványok olykor első említések az egész régióból vagy legalább az illető lelőhelyről. Magyarországról a pákozdi gránitban lévő hidrotermás ércindikációból churchit-(Y), a siroki Darnó-hegy metabázitjából pumpellyit-(Fe^{3+}) és julgoldit-(Fe^{3+}), míg az egerbaktai jura agyagpala mangános konkrécióiból chamosit vizsgálati adatait közöljük. Romániából a bánsági Tiszafa szerpentinesedett ultrabázisos magmatitjából reevesit, egy tőkési monzodioritból axinitek, míg a solymosbucsai jura üledékek mangántelepéből braunit domináns jelenlétét dokumentáljuk. Az ukrajnai Oporec melletti mezozoos homokkő repedéseiből evenkit vizsgálati adatait közöljük, mely kalcitos repedéskitöltésekből került elő szénhidrogénzárványos kvarc („máramarosi gyémánt" változat) kíséretében.

Tárgyszavak: churchit-(Y), pumpellyit-(Fe^{3+}), julgoldit-(Fe^{3+}), chamosit, reevesit, axinit, braunit, evenkit

Abstract

Further data are presented on mineral occurrences in the Carpathian–Pannonian region in this sixth instalment of the series arranged by countries and localities. Each "mosaic" contains a concise mineral description, mainly based on XRPD, SEM-EDX and EMPA measurements, and a brief characterisation of the mineral paragenesis. Some minerals are first-time descriptions from the entire discussed region, but all are newly documented occurrences from at least the described locality. From Hungary, mineralogical data are reported on churchite-(Y) from a hydrothermal ore indication in the granite near Pákozd, pumpellyite-(Fe^{3+}) and julgoldite-(Fe^{3+}) from the metabasite of the Darnó Hill in Sirok, and chamosite from manganese concretions in the Jurassic shale of Egerbakta. From Romania, the presence of the following minerals is recorded: reevesite from the serpentinized ultrabasic magmatite of Eibenthal in Banat, axinite from monzodiorite of Groşii Ţibleşului, and braunite from a manganese deposit in the Jurassic sediments of Buceava-Şoimuş. We present the data of evenkite from the fissures of Mesozoic sandstone near Oporets, Ukraine, which was found in calcite fillings in association with hydrocarbon-containing quartz ("Marmarosh diamond" variety).

Keywords: churchite-(Y), pumpellyite-(Fe^{3+}), julgoldite-(Fe^{3+}), chamosite, reevesite, axinite, braunite, evenkite

Minerals described in this paper

Table I lists the minerals described in this paper with their ideal composition, the locality where the mineral was found and also the methods, which were used for their identification. The geographical location of the discussed mineral localities is marked on a schematic geological map of the Carpathian–Pannonian region (*Figure 1*).

Experimental methods and samples

X-ray powder diffraction (XRPD) patterns of churchite-(Y), axinite, pumpellyite, chamosite and braunite were recorded on a Bruker D8 Advance diffractometer using Cu$K\alpha$ radiation (40 kV and 40 mA) with a 250 mm-radius goniometer, in parallel-beam geometry obtained by Goebel-mirror optics, 0.25° primary axial Soller with a 0.6 mm

Table I. List of identified minerals with their theoretical formulae, locality and identification method

I. táblázat. *Az azonosított ásványok ideális képletükkel, lelőhelyükkel és az azonosítás módjával*

Mineral	Ideal formula	Locality	Identification method
Axinite-(Fe)	$Ca_2Fe^{2+}Al_2BSi_4O_{15}(OH)$	Arcer adit, Groşii Ţibleşului, Ţibleş Mts., ROM	XRPD, WDX
Axinite-(Mg)	$Ca_2MgAl_2BSi_4O_{15}(OH)$	Arcer adit, Groşii Ţibleşului, Ţibleş Mts., ROM	XRPD, WDX
Axinite-(Mn)	$Ca_2Mn^{2+}Al_2BSi_4O_{15}(OH)$	Arcer adit, Groşii Ţibleşului, Ţibleş Mts., ROM	XRPD, WDX
Braunite	$Mn^{2+}Mn^{3+}{}_6SiO_{12}$	Buceava-Şoimuş, Munţii Zarandului, ROM	XRPD, WDX
Chamosite	$(Fe^{2+}, Mg)_5Al(Si_3Al)O_{10}(OH)_8$	Reszél Hill, Egerbakta, Bükk Mts., HUN	XRPD, WDX
Churchite-(Y)	$YPO_4 \cdot 2H_2O$	Sas Hill, Pákozd, Velence Hills, HUN	XRPD, WDX
Evenkite	$C_{23}H_{48}$	Beskids railway tunnel, Oporets, Eastern Beskids, UKR	XRPD, GC
Julgoldite-(Fe^{3+})	$Ca_2Fe^{3+}Fe^{3+}{}_2(SiO_4)(Si_2O_7)O(OH) \cdot H_2O$	Darnó Hill, Sirok, Mátra Mts., HUN	WDX, Mössbauer
Pumpellyite-(Fe^{3+})	$Ca_2Fe^{3+}Al_2(SiO_4)(Si_2O_7)O(OH) \cdot H_2O$	Darnó Hill, Sirok, Mátra Mts., HUN	WDX, Mössbauer
Reevesite	$Ni_6Fe^{3+}{}_2(CO_3)(OH)_{16} \cdot 4H_2O$	Eibenthal, South Banat, ROM	XRPD, WDX

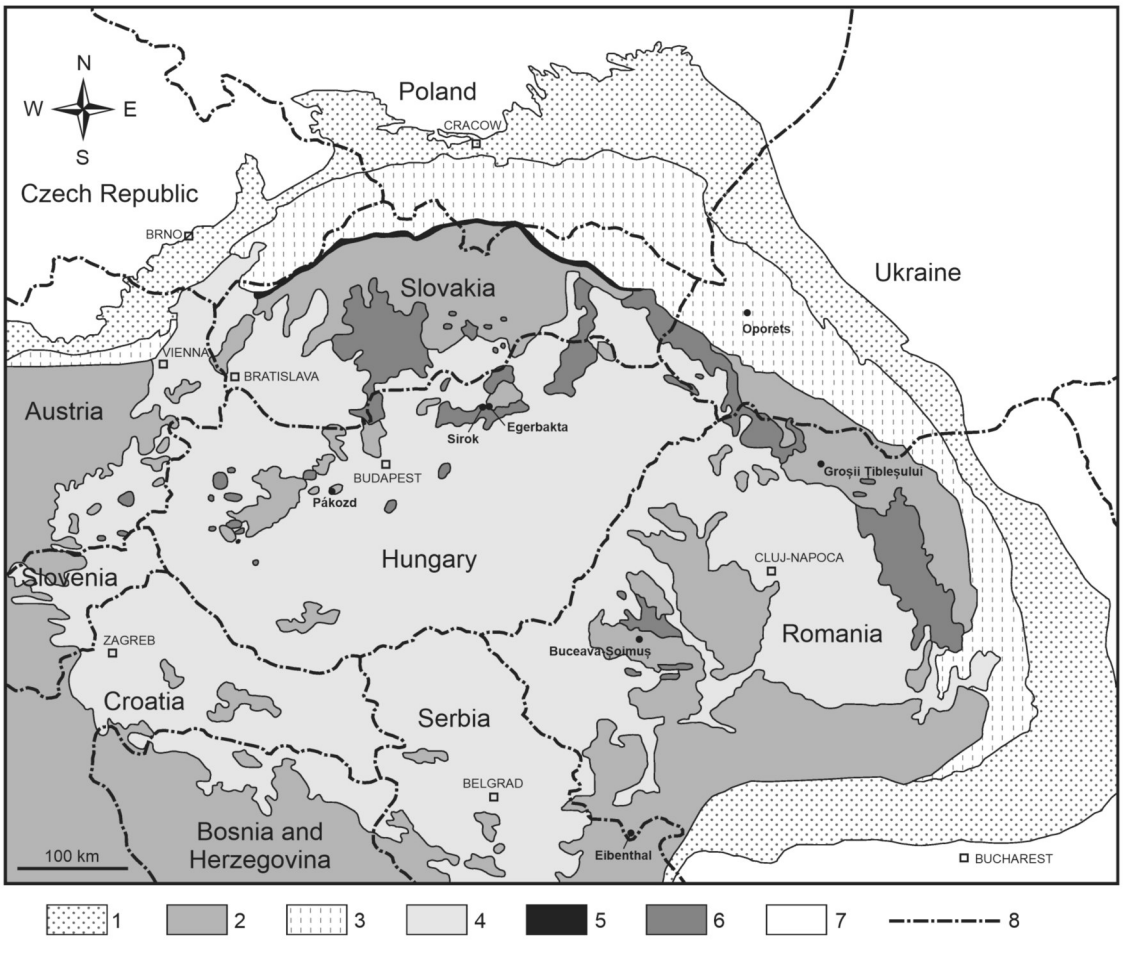

Figure 1. Location of the discussed localities marked on the schematic geological map of the Carpathian–Pannonian region.

Legend: 1 = Alpine-Carpathian foredeep; 2 = Inner Alpine, Carpathian and Dinarides units; 3 = Alpine-Carpathian flysch belt; 4 = Neogene basins; 5 = Pieniny Klippen Belt; 6 = neovolcanic areas; 7 = foreland platform areas; 8 = state borders

1. ábra. *A tárgyalt lelőhelyek elhelyezkedése a Kárpát-Pannon régió vázlatos földtani térképén.*

Jelmagyarázat: 1 = Alpi-Kárpáti előmélyedés; 2 = Belső-Alpi, Kárpáti és Dinári egységek; 3 = Alpi-Kárpáti flisöv; 4 = neogén medencék; 5 = Pienini-szirtöv; 6 = neovulkáni területek; 7 = előtéri platformterületek; 8 = országhatárok

divergence slit and position sensitive Vantec-1 detector (1° opening). Samples of 1 to 5 mg were ground in agate mortar under acetone and loaded on low-background (Si crystal) sample holders. All patterns were recorded in the 2–70° (2Θ) range with 0.007° (2Θ) / 4 sec scanning rate.

XRPD pattern was obtained for evenkite with a Philips model PW1050 Bragg-Brentano-type diffractometer using Cu*K*α radiation (40 kV, 35 mA) and a secondary graphite monochromator. The data were recorded over the 2Θ range 3–35° using 0.02° steps and a counting time of 2 s/step.

X-ray diffraction study was also performed with a 114.6 mm diameter Gandolfi camera for reevesite. Analytical parameters: Cu*K*α radiation, Ni filter, 40 kV accelerating voltage, 25 mA tube current, 44 hours exposition time. Unit cell parameters were calculated with the UnitCell software (Holland & Redfern 1997).

Scanning electron microscopy (SEM) studies and energy-dispersive X-ray spectroscopy (EDX) were done on a JEOL JXA-8600 Superprobe unit equipped with an EDX silicon drift detector (SDD) at the Institute of Exploration Geosciences, University of Miskolc. For the EDX measurements 15–20 kV accelerating voltage was used, with a probe current of 10–20 nA. A 4 × 5 μm area was scanned with a focused beam during the analyses (stopped focused beam was used if the target area was too small).

Quantitative electron-microprobe analyses (EMPA) were performed at the Geological Institute of Dionýz Štúr, Bratislava, Slovakia. For the analyses of churchite-(Y), pumpellyite-(Fe^{3+}), julgoldite-(Fe^{3+}), chamosite, reevesite, axinite and braunite, a Cameca SX-100 instrument was used in wavelength-dispersive mode (WDX). Operating conditions were as follows: accelerating voltage 15 kV, probe current 20 nA. Analytical standards: baryte (S), apatite (P), GaAs (As), SiO_2 (Si), TiO_2 (Ti), Al_2O_3 (Al), Cr_2O_3 (Cr), fayalite (Fe), YPO_4 (Y), $REEPO_4$ (REEs), MgO (Mg), wollastonite (Ca), rhodonite (Mn), Co (Co), Ni (Ni), albite (Na), orthoclase (K), CaF_2 (F) and NaCl (Cl). Raw intensity data were corrected using a PAP matrix correction.

The ^{57}Fe Mössbauer spectrum of pumpellyite-julgoldite was recorded at HUN-REN Centre for Energy Research on a spectrometer assembly produced by KFKI, Hungary. 1 GBq ^{57}Co radiation source was used in constant acceleration mode. Counts were collected in 1000 channels; the evaluated 500 channel spectrum was obtained after folding of the two halves of the primary recording. The isomer shift values are relative to the center of the metallic alpha-iron spectrum, the accuracy of the measured values is ± 0.03 mm/s. The spectrum was evaluated as a superposition of Lorentz distributions, there were no constrained parameters in the evaluation.

Chromatographic analysis of evenkite was carried out with a Shimadzu Nexis GC-2030 chromatograph using flame ionization detector (FID). The instrument was equipped with a Zebron ZB-1HT Inferno fused silica column, 30 m long, with an internal diameter of 0.32 mm. The inner walls of the column were coated with a stationary phase, its layer thickness was 0.25 μm. The sample concentration was 1 mg/ml, of which 1 μl was injected for measurement. The injector was operated in splitless mode. The temperatures of the injector and the detector were 290 °C and 390 °C, respectively. The initial oven temperature was set at 50 °C for 2 min, after which it was ramped to 390 °C at 8 °C/min. The column was held at the final temperature of 390 °C for 4.5 min.

All investigated samples are deposited in the mineral collection of the Herman Ottó Museum, Miskolc, Hungary (inventory numbers: 2023.35 for churchite-(Y), Pákozd; 2016.422 and 23045 for pumpellyite and julgoldite, Sirok; 2020.104 for chamosite, Egerbakta; 2024.8 for reevesite, Eibenthal; 2023.15 for axinite, Groşii Ţibleşului; 2024.137 for braunite, Buceava-Şoimuş; and 2020.159 for evenkite, Oporets). A few braunite samples were also studied from the collection of Supervisory Authority of Regulatory Affairs (MÁFI – AT 185.1).

Results

Hungary

Churchite-(Y) from Sas Hill, Pákozd, Velence Hills

A diverse mineral assemblage has been detected in the hydrothermal ore indication in the highly silicified zones in the lineament from the Sas Hill to the Ősi Hill, near Pákozd. Here, secondary phases formed from sulphides [predominantly galena, tennantite-(Zn), tennantite-(Fe), pyrite] represent new data: pyromorphite, less commonly mimetite as white or brown, hexagonal columnar or acicular crystals; cerussite as colourless or grey, dipyramidal and tabular crystals; azurite as blue coatings, less commonly mm-sized tablets; malachite as green crusts, fibres, needles, worm-like clusters or spheres; mixite as pale green, acicular-radial aggregates; wulfenite as orange, tabular crystals; chrysocolla as pale blue encrustations; carminite as red-brown, acicular-radial aggregates; segnitite as brown or yellowish, sub-mm rhombohedra; pharmacosiderite as yellow, cubic crystals; conichalcite as greenish crusts; arseniosiderite as brown, globular clusters; coronadite as black crusts and porous clusters; intimately intergrown ramsdellite and groutite as black, spherical aggregates; and cinnabar as red, powdery aggregates. Each phase occurs in sizes of around 1–3 mm.

The most interesting mineral, however, is a water-containing yttrium phosphate ($YPO_4 \bullet 2H_2O$), churchite-(Y), observed as white or butter-coloured needles in radiating or spherical aggregates reaching 0.1–0.3 mm in diameter (*Figure 2*). It was determined by X-ray powder diffraction (*Table E1* – see the electronic supplementary materials) and electron-microprobe analyses (*Table II*). The latter suggests that churchite-(Y) is chemically quite homogeneous, with some variation only in the Ca/REE ratio. Among REEs, heavy REEs dominate, such as Dy, Er and Gd. Note that the water content calculated from the ideal formula for churchite-(Y) is 16.39 wt%, which is much higher than the difference between the analytical totals and 100% (6.22–11.61 wt%). This

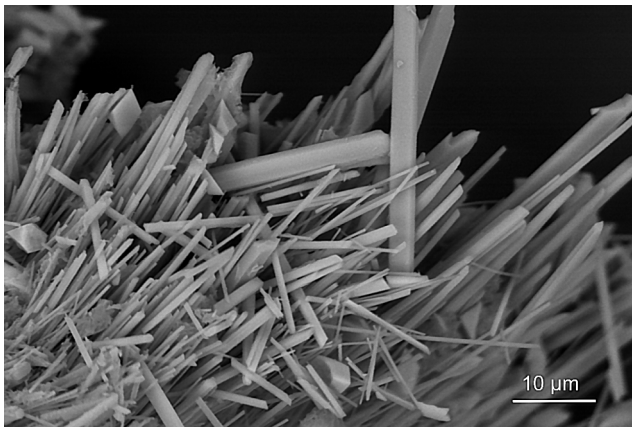

Figure 2. Acicular crystals of churchite-(Y), Pákozd. BSE image. Photo courtesy of Á. KOVÁCS

2. ábra. *Tűs churchit-(Y)-kristályok, Pákozd. Visszaszórtelektron-kép. Fotó: KOVÁCS Á.*

suggests that varying amounts of water were removed from the mineral during the analyses, and therefore the water content of churchite cannot be estimated from the analytical data. Unit cell parameters of the mineral calculated from XRPD data are $a = 5.574(4)$, $b = 14.961(7)$, $c = 6.284(4)$ Å, $\beta = 117.85(5)°$ and $V = 463.4(4)$ Å^3 (space group $A2/a$).

REE-containing phases (keralite and monazite) are reported in both the decomposed granite and the siliceous veins of the Ősi Hill by B. KISS et al. (2024). The presence of phosphorus and REE is explained by mobilization by fluids associated with hydrothermal processes. The formation of churchite-(Y) is also likely to have been contributed by the REE-bearing accessory phases in the granite.

Pumpellyite-(Fe^{3+}) and julgoldite-(Fe^{3+}) from Darnó Hill, Sirok, Mátra Mts.

On Darnó Hill, FÖLDESSY (1975) first identified pumpellyite as a characteristic component of metabasites that underwent prehnite-pumpellyite facies metamorphism. He found quartz, calcite, clinochlore and epidote in the vein fillings of the metabasites together with pumpellyite. More recently, B. KISS et al. (2016) examined in detail the phases formed by hydrothermal alteration in the Triassic magmatites of the area. They found that pumpellyite formed together with prehnite. Among the rock-forming minerals, clinopyroxenes (augite, diopside) are the most common, with minor amounts of apatite, albite, titanite and spinel (JÓZSA 1999).

However, pumpellyite is not the name of a species, but of a mineral group with the general formula $W_2XY_2Z_3O_{14-n}(OH)_n$, where W = Ca; X = Mg, Mn^{2+}, Fe^{2+}, Fe^{3+}, Al, V^{3+}, Cr^{3+}; Y = Al, Fe^{3+}, Mn^{3+}, V^{3+}, Cr^{3+}; Z = Si and n = 3–4. Pumpellyite group is divided into five subgroups after the most dominant Y-site cation, i.e. pumpellyite (Y = Al), julgoldite (Y = Fe^{3+}), okhotskite (Y = Mn^{3+}), poppiite (Y = V^{3+}) and shuiskite subgroup (Y = Cr^{3+}) (NAGASHIMA et al. 2006). Within each subgroup, mineral species are defined by the dominant cation in the X-site. The names of mineral species are formed by placing the chemical symbol of the dominant X-cation in parentheses after the name of the subgroup, e.g., pumpellyite-(Al).

Table II. Electron-microprobe analyses of churchite-(Y) from the Sas Hill, Pákozd, Hungary, in wt%

II. táblázat. *A sas-hegyi (Pákozd) churchit-(Y) elektronmikroszondás elemzései tömegszázalékban*

	(1)	(2)	(3)	(4)	(5)
SO_3	0.04	0.00	0.10	0.04	0.06
P_2O_5	31.11	31.52	30.76	30.24	30.29
As_2O_5	0.01	0.00	0.02	0.00	0.00
Y_2O_3	38.62	39.15	41.82	37.68	36.29
La_2O_3	0.46	0.50	0.19	0.57	0.56
Ce_2O_3	1.90	1.76	0.54	1.99	2.23
Pr_2O_3	0.32	0.45	0.11	0.44	0.57
Nd_2O_3	2.99	2.79	1.20	2.78	3.32
Sm_2O_3	1.47	1.37	0.58	1.41	1.54
Eu_2O_3	0.52	0.47	0.27	0.43	0.56
Gd_2O_3	3.65	3.43	1.87	3.46	3.75
Tb_2O_3	0.73	0.73	0.39	0.90	0.73
Dy_2O_3	5.21	5.16	3.47	5.11	5.19
Ho_2O_3	0.98	1.00	0.72	1.03	0.89
Er_2O_3	3.31	3.27	2.79	3.27	3.09
Tm_2O_3	0.39	0.40	0.29	0.45	0.31
Yb_2O_3	1.38	1.24	1.06	1.29	1.25
Lu_2O_3	0.25	0.07	0.09	0.05	0.13
CaO	0.37	0.38	2.08	0.54	0.37
FeO*	0.04	0.06	0.01	0.05	0.02
Total	**93.76**	**93.78**	**88.39**	**91.72**	**91.14**
Cation numbers based on 4 oxygens Kationszámok 4 oxigénre					
S	0.00	0.00	0.00	0.00	0.00
P	0.97	0.97	0.97	0.96	0.97
As	0.00	0.00	0.00	0.00	0.00
Σ*T*	**0.97**	**0.97**	**0.97**	**0.96**	**0.97**
Y	0.75	0.76	0.83	0.75	0.73
La	0.01	0.01	0.00	0.01	0.01
Ce	0.03	0.02	0.01	0.03	0.03
Pr	0.00	0.01	0.00	0.01	0.01
Nd	0.04	0.04	0.02	0.04	0.04
Sm	0.02	0.02	0.01	0.02	0.02
Eu	0.01	0.01	0.00	0.01	0.01
Gd	0.04	0.04	0.02	0.04	0.05
Tb	0.01	0.01	0.00	0.01	0.01
Dy	0.06	0.06	0.04	0.06	0.06
Ho	0.01	0.01	0.01	0.01	0.01
Er	0.04	0.04	0.03	0.04	0.04
Tm	0.00	0.00	0.00	0.01	0.00
Yb	0.02	0.01	0.01	0.01	0.01
Lu	0.00	0.00	0.00	0.00	0.00
Ca	0.01	0.01	0.08	0.02	0.01
Fe	0.00	0.00	0.00	0.00	0.00
Σ*A*	**1.05**	**1.05**	**1.06**	**1.07**	**1.04**

* Total iron was measured as FeO / *Összes vas FeO-ként mérve*

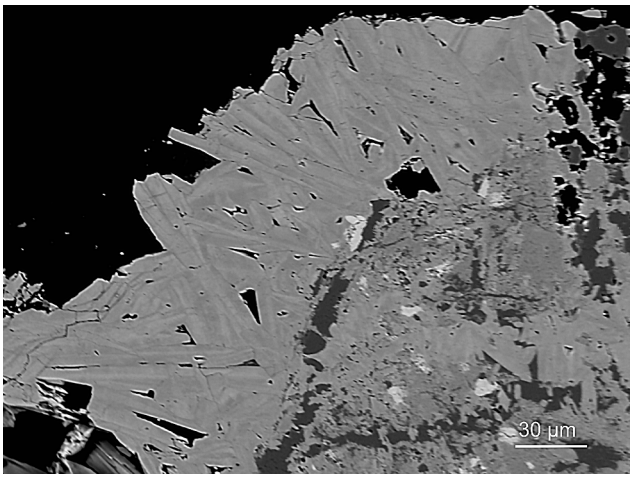

Figure 3. Chemically zoned, columnar pumpellyite-julgoldite crystals, Sirok. BSE image. Photo courtesy of V. KOLLÁROVÁ

3. ábra. *Kémiailag zónás, oszlopos pumpellyit-julgolditkristályok, Sirok. Visszaszórt-elektron-kép. Fotó: V. KOLLÁROVÁ*

Table III. Electron-microprobe analyses of pumpellyite-group minerals from Darnó Hill, Sirok, Hungary (in wt.%)

III. táblázat. *A pumpellyit-csoportba tartozó ásványok elektronmikroszondás elemzései a siroki Darnó-hegyről tömegszázalékban*

	(1)	(2)	(3)	(4)	(5)	(6)
SiO_2	33.15	32.83	34.86	36.19	35.77	36.02
TiO_2	0.00	0.04	0.06	0.03	0.06	0.04
Al_2O_3	3.45	2.87	11.36	18.13	15.76	19.41
Cr_2O_3	0.01	0.00	0.00	0.00	0.01	0.00
Fe_2O_3*	33.23	36.06	25.15	15.57	18.93	13.45
MgO	1.92	0.97	1.24	1.93	1.82	1.75
CaO	20.59	20.41	21.44	22.39	22.20	22.11
MnO	0.77	0.43	0.21	0.08	0.07	0.02
FeO*	1.20	1.30	0.91	0.57	0.68	0.49
NiO	0.00	0.00	0.00	0.00	0.00	0.02
Na_2O	0.04	0.01	0.00	0.02	0.04	0.00
K_2O	0.01	0.00	0.00	0.01	0.00	0.00
H_2O**	5.65	5.40	5.60	5.95	5.90	5.80
Total	**99.97**	**100.32**	**100.83**	**100.87**	**101.24**	**99.11**
Ion numbers based on 14 (O, OH) anions Ionszámok 14 (O, OH) anionra						
Si	2.99	2.98	3.00	2.99	2.99	3.01
Al	0.01	0.02	0.00	0.01	0.01	0.00
Σ*Z*	**3.00**	**3.00**	**3.00**	**3.00**	**3.00**	**3.01**
Al	0.36	0.29	1.15	1.76	1.54	1.91
Fe^{3+}	1.64	1.71	0.85	0.24	0.46	0.09
Σ*Y*	**2.00**	**2.00**	**2.00**	**2.00**	**2.00**	**2.00**
Cr^{3+}	0.00	0.00	0.00	0.00	0.00	0.00
Fe^{3+}	0.61	0.75	0.78	0.73	0.73	0.76
Mg	0.26	0.13	0.16	0.24	0.23	0.22
Mn	0.06	0.03	0.02	0.01	0.00	0.00
Fe^{2+}	0.09	0.10	0.07	0.04	0.05	0.03
Ni	0.00	0.00	0.00	0.00	0.00	0.00
Σ*X*	**1.02**	**1.01**	**1.03**	**1.02**	**1.01**	**1.01**
Ca	1.99	1.98	1.98	1.98	1.99	1.98
Na	0.00	0.00	0.00	0.00	0.01	0.00
K	0.00	0.00	0.00	0.00	0.00	0.00
Σ*W*	**1.99**	**1.98**	**1.98**	**1.98**	**2.00**	**1.98**
O	10.60	10.73	10.79	10.72	10.71	10.77
OH	3.40	3.27	3.21	3.28	3.29	3.23
mineral/ ásvány***	Jul-(Fe^{3+})	Jul-(Fe^{3+})	Pmp-(Fe^{3+})	Pmp-(Fe^{3+})	Pmp-(Fe^{3+})	Pmp-(Fe^{3+})

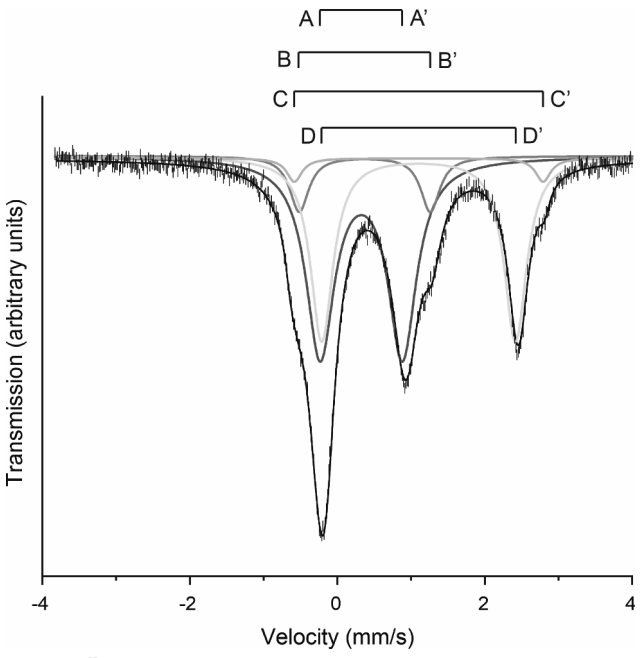

Figure 4. ^{57}Fe Mössbauer spectrum of pumpellyite-julgoldite contamined with chlorite from Sirok

4. ábra. *Klorittal szennyezett pumpellyit-julgoldit ^{57}Fe Mössbauer-spektruma, Sirok*

Since the exact classification according to the above nomenclature has not yet been carried out on species level, electron-microprobe analyses and Mössbauer spectroscopic study were performed on the Sirok pumpellyite. The prismatic crystals of pumpellyite, sometimes reaching 1 mm, appearing in the cracks of the decomposed metabasalt, are located in a quartz-albite matrix. It can be observed in the BSE images that the crystals show chemical zoning (*Figure 3*). Based on the microprobe analyses (*Table III*), in the lighter zones Fe (julgoldite subgroup), while in the darker zones Al is the dominant *Y*-cation (pumpellyite subgroup). For the species-level classification, the valence state of iron still had to be clarified. If we calculate the formula based on $O_{11}(OH)_3$ from the analyses, assuming all iron to be trivalent, then we get a slight cation excess (8.05–8.11 apfu) compared to the ideal 8 apfu, which suggests that the mineral contains no or only a very small amount of divalent iron, since its increasing proportion would further increase the total cation number. This was also confirmed by Mössbauer spectroscopic analysis (*Figure 4* and *Table IV*), where the Fe^{3+}:Fe^{2+} ratio was found to be about 96:4. The valence state and crystal structure position of the iron belonging to each doublet were determined according to AKASAKA et al. (1997). The D-D' doublet (*Figure 4*), indicating a large amount of Fe^{2+}, originates from chlorite contamination in the examined sample. The values IS = 1.15 mm/s and QS = 2.62 mm/s clearly refer to Fe^{2+} in the octahedral sites of chlorite (see e.g., DE GRAVE et al. 1987). According to AKASAKA et al.

← *Total iron was measured as Fe_2O_3. Fe^{3+}/Fe^{2+} was calculated from Mössbauer spectroscopy. / *Összes vas Fe_2O_3-ként mérve. Fe^{3+}/Fe^{2+} a Mössbauer-spektroszkópiából számolva.*

← **H_2O calculated from the stoichiometry: total cations = 8 apfu / *H_2O a sztöchiometrikus összetételből számolva: összes kation = 8 apfu.*

← ***Jul = julgoldite / *julgoldit*, Pmp = pumpellyite / *pumpellyit*.

Table IV. ^{57}Fe Mössbauer hyperfine parameters of pumpellyite-julgoldite from Sirok
IV. táblázat. *A siroki pumpellyit-julgoldit hiperfinom ^{57}Fe Mössbauer paraméterei*

Doublet* Dublett*	Isomer shift (IS) Izomér eltolódás (mm/s)	Quadrupole splitting (QS) Kvadrupól felhasadás (mm/s)	Area ratio Területarány (%)	Assignment Jelölés
A–A'	0.34	1.18	52.2	$^{X}Fe^{3+}$
B–B'	0.37	1.83	10.0	$^{Y}Fe^{3+}$
C–C'	1.09	3.44	2.5	$^{X}Fe^{2+}$
D–D'	1.15	2.62	35.3	Fe^{2+} in chlorite

* Abbreviations of doublets are the same as those in Figure 4. / *A dublettek rövidítései ugyanazok, mint a 4. ábrán.*

(1997), such values also represent Fe^{2+} in the *W*-site in pumpellyite, but this position is essentially entirely filled by calcium, here Fe^{2+} can only be present in traces.

The Fe^{3+}:Fe^{2+} ratio presented in *Table III* was calculated from Mössbauer study, while the water content was calculated such that the number of total cations was 8 apfu. Thus, the amount of OH ranged between 3.21 and 3.40 apfu. Since the dominant *X*-cation in all analyses is Fe^{3+}, the Sirok specimen represents pumpellyite-(Fe^{3+}) and julgoldite-(Fe^{3+}) species, depending on the dominant *Y*-cation. The distribution of Fe^{3+} between the *X* and *Y* sites based on Mössbauer spectroscopy is approximately 5:1, but this value is not meaningful in the case of the examined sample due to its large chemical variability; it can be considered as a kind of average and perhaps indicates the dominance of the pumpellyite composition compared to julgoldite.

Chamosite from Reszél Hill, Egerbakta, Bükk Mts.

A few years ago, manganese-containing concretions were found in Jurassic shales in an abandoned quarry on the Reszél Hill, near Egerbakta. The spherical concretions are between 5 and 15 cm in diameter and are encrusted by a relatively hard black material, mainly composed of Mn oxides. Their XRPD pattern confirmed the presence of poorly crystalline phases with some todorokite. The core of the concretions has a coarse-grained texture and, according to the XRPD patterns, consists of iron-rich chlorite, quartz and illite. Among the members of the mineral assemblage, the iron-rich chlorite was studied in more detail. Some microprobe analyses were performed (*Table V*), which show that this phase corresponds to chamosite within the chlorite group. All iron was measured as FeO; the presence of Fe^{3+} was not taken into account, since the cation content of the octahedral sites does not reach the ideal 6 apfu (varying between 5.80 and 5.91 apfu), and increasing the Fe^{3+}:Fe^{2+} ratio would further increase the cation deficiency.

The 10–70 μm-sized, lenticular or spherical aggregates of chamosite are located between the iron oxide-impregnated, bent illite flakes and the equant grains of quartz (*Figure 5*). Due to the alteration of illite and chamosite, the concretions in some zones are very porous, with a cellular texture, and are made up of quartz aggregates. The BSE images also clearly show how the rims of the chamosite aggregates have been transformed into Mn-oxides in some places. There are zones where the transformation is not significant and there are areas, such as the rims of larger concretions, where only Mn-oxides can be found (with some iron-oxides). The formation of chamosite concretions can be related to ocean-floor metamorphism, taking into account the geological structure of the local environment. According to B. KISS et al. (2016), the chlorites of the ocean-floor magmatites of the wider area appear in great chemical and morphological diversity and are abundant components of hydrothermal formations. Microprobe analyses of these chlorites reveal Fe-

Table V. Electron-microprobe analyses of chlorite from Egerbakta in wt%
V. táblázat. *Az egerbaktai klorit elektronmikroszondás elemzései tömegszázalékban*

	(1)	(2)	(3)
SiO_2	24.73	23.91	23.28
TiO_2	0.00	0.02	0.00
Al_2O_3	22.66	22.74	22.45
MgO	4.83	4.36	4.32
CaO	0.06	0.01	0.06
MnO	1.17	1.81	1.89
FeO*	34.85	35.50	36.40
NiO	0.02	0.02	0.00
Na_2O	0.00	0.00	0.04
K_2O	0.01	0.01	0.01
H_2O**	10.88	10.78	10.69
Total	**99.21**	**99.16**	**99.15**
Ion numbers based on 18 (O, OH) anions Ionszámok 18 (O, OH) anionra			
Si	2.73	2.66	2.61
Al	1.27	1.34	1.39
Σ*T*	**4.00**	**4.00**	**4.00**
Ti	0.00	0.00	0.00
Al	1.67	1.64	1.58
Mg	0.79	0.72	0.72
Ca	0.01	0.00	0.01
Mn	0.11	0.17	0.18
Fe^{2+}	3.21	3.30	3.41
Ni	0.00	0.00	0.00
Na	0.00	0.00	0.01
K	0.00	0.00	0.00
Σ*M*	**5.80**	**5.85**	**5.91**
O	10.00	10.00	10.00
OH	8.00	8.00	8.00

Other measured, but undetected elements: Cr, F and Cl. / *Egyéb mért, de nem detektált elemek: Cr, F és Cl.*
* Total iron was measured as FeO. / *Összes vas FeO-ként mérve.*
** H_2O calculated from the stoichiometry: OH = 8 apfu. / *H_2O a sztöchiometrikus összetételből számolva: OH = 8 apfu.*

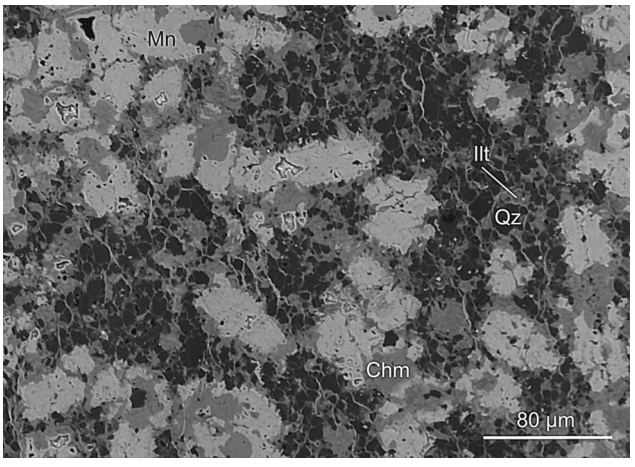

Figure 5. BSE image of a chamosite-bearing concretion, Egerbakta.
Abbreviations: Chm = chamosite, Ilt = illite, Mn = undefined Mn-oxide, Qz = quartz

5. ábra. *Egy chamositos konkréció visszaszórtelektron-képe, Egerbakta.*
Rövidítések: Chm = chamosit, Ilt = illit, Mn = meghatározatlan Mn-oxid, Qz = kvarc

rich clinochlore to be common, in some deposits (e.g., on the Nagy-Réz-side of Recsk) to such an extent that the Mg:Fe cation ratio shows a value of around 2.5:2, which is not far from the clinochlore-chamosite boundary. Furthermore, B. Kiss et al. (2024) place the process of illite transformation at the last stage of hydrothermal rock alteration. This may have happened in the case of the examined concretions as well, because the chamosite formed in the first stage is replaced by illite in the rock during further transformation processes. The released iron and manganese ions of the weathered chamosite precipitated later as oxide and oxyhydroxide phases.

Romania

Reevesite from Eibenthal (Tiszafa), South Banat

In the ophiolite series around Eibenthal (South Banat), mainly in serpentinites, green, yellow and purple, secondary crusts or film-like precipitates are found in connection with the nickel and chromium enrichments of the area. According to Strusievicz (1995), the green coatings and crusts are mixtures of theophrastite and nimite. Earlier authors also mentioned them as garnierite (e.g., Savul 1932), which according to today's nomenclature is a mixture of secondary Ni-containing components.

In the present study, we focus on the yellow secondary phase. Lemon-yellow, film-like coatings or powdery aggregates appear both in the chromium ore once mined at Goleţu Mare, encrusting the chromite grains, and in the cracks of serpentinite around Eibenthal. The excavations providing the best samples were established during the widening of the road along the Danube around 2010. According to SEM images, these coatings are loosely joined clusters consisting of 2–6 µm-sized, bent flakes (*Figure 6*), which form crusts or powdery aggregates. Hexagonal tabular crystals of similar size can also be observed rarely. According to the XRPD

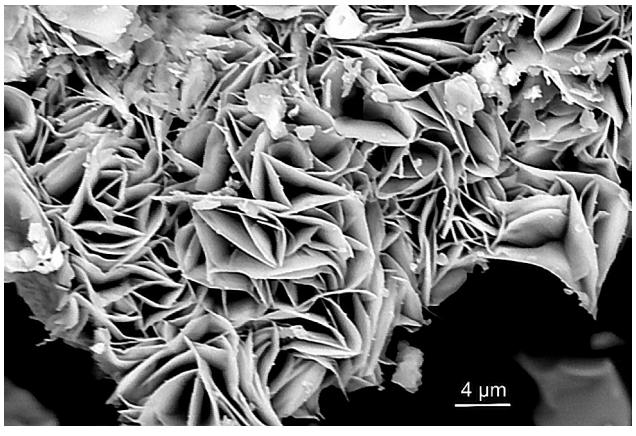

Figure 6. Bent flakes of reevesite, Eibenthal. BSE image. Photo courtesy of Á. Kovács

6. ábra. *Reevesit hajlott pikkelyei, Tiszafa. Visszaszórtelektron-kép. Fotó: Kovács Á.*

data (*Table E2* – see the electronic supplementary materials) and WDX analyses (*Table VI*), this phase can be identified as reevesite, which is a trigonal, hydrous nickel-iron-carbonate-hydroxide: $Ni_6Fe^{3+}_2(CO_3)(OH)_{16} \bullet 4H_2O$. Unit cell parameters of the mineral calculated from XRPD data are $a = 6.11(3)$, $c = 45.5(1)$ Å and $V = 1472(12)$ Å^3 (space group $R\text{–}3m$). From the chemical analyses, an elevated Mg content

Table VI. Electron-microprobe analyses of reevesite from Eibenthal, Romania (in wt.%)

VI. táblázat. *A reevesit elektronmikroszondás elemzései Tiszafáról tömegszázalékban*

	(1)	(2)	(3)
CO_2*	5.40	5.45	5.30
SiO_2	0.16	0.34	0.08
Fe_2O_3**	19.75	19.61	18.75
MgO	6.36	8.46	5.26
MnO	0.06	0.49	0.09
CoO	0.06	0.45	0.11
NiO	41.99	38.29	44.27
H_2O***	26.37	26.84	25.99
Total	**100.16**	**99.94**	**99.87**
Ion numbers based on 19 oxygens Ionszámok 19 oxigénre			
C	1.00	1.00	1.00
Si	0.02	0.05	0.01
Fe^{3+}	2.03	1.98	1.95
Mg	1.29	1.69	1.09
Mn	0.01	0.06	0.01
Co	0.01	0.05	0.01
Ni	4.61	4.13	4.93
OH	16.00	16.00	16.00

* CO_2 calculated from the stoichiometry: C = 1 apfu / *CO_2 a sztöchiometrikus összetételből számolva: C = 1 apfu*
** Total iron calculated as Fe_2O_3. / *Összes vas Fe_2O_3-ként számolva.*
*** H_2O calculated from the stoichiometry: 16 (OH) plus 4 (H_2O) / *H_2O a sztöchiometrikus összetételből számolva: 16 (OH) + 4 (H_2O)*

can be highlighted. Reevesite is certainly the alteration product of pentlandite, a Ni-containing sulfide present in serpentinite, which is common in small amounts. In its close paragenesis, minerals of the rosasite group can often be observed, among which Ni-containing glaukosphaerite, mcguinnessite, malachite, rosasite, and an unknown Ni-Mg-containing rosasite can be detected (FEHÉR et al. 2010).

Axinite minerals from Arcer adit, Groşii Ţibleşului (Tőkés), Ţibleş Mts.

Mg-rich skarn formations, associated with monzodiorite, were first identified in the area by UDUBAŞA et al. (1982). They occurred in several excavations in the research adits below Arcer Peak. The axinite samples we examined were found in the large waste heap that accumulated the material of the Arcer adits in the late 1970s. The axinite, reaching 1–3 mm in size, colourless or white, with characteristic chisel-shaped crystals, can be observed on the walls of cracks in rocks showing significant weathering. The determination was made based on XRPD data and WDX analyses. Based on the BSE images, the crystals show chemical zoning (*Figure 7*), where the darker zones are richer in Mg, while the dominant, lighter areas are Fe- and Mn-rich. Based on the dominant cation in the "*Y*" site, three species can be identified, namely axinite-(Fe), axinite-(Mn) and axinite-(Mg) (*Table VII*). Due to the Mg enrichment of the environment, the presence of Mg-dominant axinite, which is a rare mineral worldwide, is not surprising. The chemically diverse axinite of the Ţibleş Mountains can be considered a low-temperature post-magmatic mineral, as also indicated by the presence of elongated, prismatic quartz crystals, the hydrothermally decomposed host rock and the fracture-filling nature of axinite. The accompanying phases, in addition to the dominant quartz, are apatite, titanite and clinochlore.

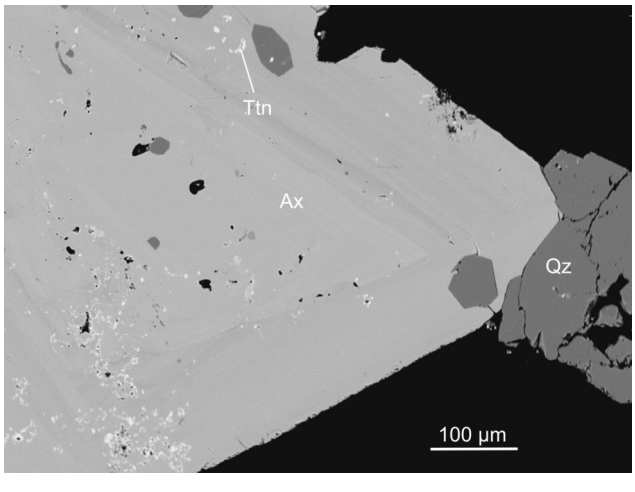

Figure 7. Chemically zoned axinite from Arcer adit, Groşii Ţibleşului. BSE image.

Abbreviations: Ax = axinite, Qz = quartz and Ttn = titanite. Photo courtesy of V. KOLLÁROVÁ

7. ábra. *Kémiailag zónás axinit, Arcser-táró, Tőkés. Visszaszórtelektron-kép. Rövidítések: Ax = axinit, Qz = kvarc és Ttn = titanit. Fotó: V. KOLLÁROVÁ*

Table VII. Electron-microprobe analyses of axinite from Groşii Ţibleşului (Romania) in wt%

VII. táblázat. *A tőkési (Románia) axinit elektronmikroszondás elemzései tömegszázalékban*

	(1)	(2)	(3)	(4)	(5)	(6)
SiO_2	43.42	42.54	43.02	43.15	43.57	42.89
TiO_2	0.03	0.02	0.01	0.00	0.00	0.00
B_2O_3*	6.30	6.25	6.27	6.27	6.30	6.27
Al_2O_3	18.42	18.72	18.53	18.18	18.61	18.36
Cr_2O_3	0.04	0.00	0.00	0.03	0.03	0.00
Fe_2O_3**	0.00	1.00	1.00	0.50	0.30	1.00
MgO	1.66	1.58	2.25	1.07	3.67	1.40
CaO	19.82	20.32	20.27	20.96	20.53	20.24
MnO	4.84	5.76	3.90	3.04	1.94	6.45
FeO**	5.63	3.22	4.51	6.71	4.16	3.23
Na_2O	0.00	0.00	0.00	0.03	0.00	0.00
K_2O	0.00	0.01	0.00	0.00	0.00	0.00
H_2O***	1.62	1.62	1.62	1.62	1.64	1.62
Total	**101.77**	**101.05**	**101.40**	**101.55**	**100.79**	**101.47**
Ion numbers based on 16 (O, OH) anions Ionszámok 16 (O, OH) anionra						
Si	4.00	3.94	3.96	3.99	3.99	3.97
Al	0.00	0.06	0.04	0.01	0.01	0.03
Σ*T*	**4.00**	**4.00**	**4.00**	**4.00**	**4.00**	**4.00**
B	1.00	1.00	1.00	1.00	1.00	1.00
Σ*B*	**1.00**	**1.00**	**1.00**	**1.00**	**1.00**	**1.00**
Al	2.00	1.99	1.97	1.97	2.00	1.97
Cr	0.00	0.00	0.00	0.00	0.00	0.00
Fe^{3+}	0.00	0.01	0.03	0.03	0.00	0.03
Σ*Z*	**2.00**	**2.00**	**2.00**	**2.00**	**2.00**	**2.00**
Fe^{3+}	0.00	0.06	0.04	0.00	0.02	0.04
Mg	0.23	0.22	0.31	0.15	0.50	0.19
Ca	0.00	0.02	0.00	0.09	0.01	0.01
Mn	0.34	0.45	0.30	0.24	0.15	0.51
Fe^{2+}	0.43	0.25	0.35	0.52	0.32	0.25
Σ*Y*	**1.00**	**1.00**	**1.00**	**1.00**	**1.00**	**1.00**
Ca	1.96	2.00	2.00	1.99	2.00	2.00
Mn	0.04	0.00	0.00	0.00	0.00	0.00
Na	0.00	0.00	0.00	0.01	0.00	0.00
K	0.00	0.00	0.00	0.00	0.00	0.00
Σ*X*	**2.00**	**2.00**	**2.00**	**2.00**	**2.00**	**2.00**
OH	1.00	1.00	1.00	1.00	1.00	1.00

Other measured, but undetected elements: Ni, F and Cl. / *Egyéb mért, de nem detektált elemek: Ni, F és Cl.*

* B_2O_3 calculated from the stoichiometry: B = 1 apfu. / *B_2O_3 a sztöchiometrikus összetételből számolva: B = 1 apfu.*

** Total iron was measured as FeO. FeO/Fe_2O_3 ratio calculated from the stoichiometry: ∑(T+B+Z+Y+X) = 10 apfu. / *Összes vas FeO-ként mérve. A FeO/Fe_2O_3 arány a sztöchiometrikus összetételből számolva: ∑(T+B+Z+Y+X) = 10 apfu.*

*** H_2O calculated from the stoichiometry: OH = 1 apfu. / *H_2O a sztöchiometrikus összetételből számolva: OH = 1 apfu.*

Braunite-dominated manganese mineralization from Buceava-Şoimuş (Solymosbucsa), Munţii Zarandului

High-grade manganese ore deposits, associated with Jurassic limestones and radiolarites, were formed related to ocean-floor basic volcanics. The ore deposits were mined in the Buceava-Şoimuş area in small-scale operations in the 19th century. An old hydro-powered manganese ore grinding mill still stands near the village. According to previous literature, psilomelane and pyrolusite constitute the bulk of the ore material (NAGY 1958). However, our more recent studies show that braunite is the dominant phase. Based on XRPD and EDX analyses, the ore minerals (in decreasing order of abundance) are braunite, cryptomelane, romanèchite, ranciéite and goethite, associated with calcite, baryte and clinochlore. The studied samples come partly from the historical collection of the Supervisory Authority for Regulatory Affairs of Hungary (Budapest) and partly from our own field collection. The ores predominantly form compact masses, to a lesser extent with a vesicular-spongy texture. Thin Mn-oxide veins, which consist purely of braunite, can often be observed in the accompanying radiolarite. In the cavities of the compact ore material, braunite is present as tetragonal dipyramidal crystals, while cryptomelane and romanèchite form acicular aggregates, lawn-like encrustations, occasionally spherical or radial aggregates, where the crystals are sub-mm in size (*Figures 8* and *9*). Ranciéite is a weathering product of the previously mentioned phases, forming brown film-like coatings. Pyrolusite described earlier has not been detected so far. The braunite is chemically homogeneous according to the WDX analyses, where 0.16–0.23 apfu Ca replacing Mn^{2+}, 0.04–0.21 apfu Al and 0.04–0.45 apfu Fe^{3+} replacing Mn^{3+} compared to the ideal $Mn^{2+}Mn^{3+}{}_6SiO_{12}$ composition (*Table VIII*). In the fracture fillings of the ore material, quartz forms 1–3 mm stubby, columnar crystals, calcite forms 1–2 mm rhombohedrons, while baryte forms tabular crystals around mm in size. A small amount of clinochlore with minor iron content can be observed as white, waxy nests. So far, only one occurrence similar to this interesting braunite-dominant manganese ore deposit is known in the Carpathian–Pannonian region, namely the Telekes Valley of Varbóc (Aggtelek-Rudabánya Mountains, Hungary). The very similar paragenesis and the texture of the ores suggest similar origin, although the Varbóc occurrence is mainly accompanied by Mesozoic limestone. However, it should be noted that radiolarite also occurs here, and ocean-floor magmatites in its wider environment (NÉMETH et al. *in prep.*).

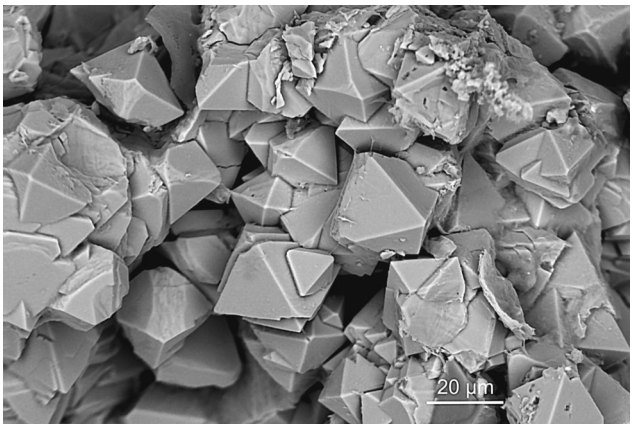

Figure 8. Dipyramidal crystals of braunite from Buceava-Şoimuş. BSE image. Photo courtesy of Á. KOVÁCS

8. ábra. *A solymosbucsai braunit dipiramisos kristályai. Visszaszórtelektron-kép. Fotó: KOVÁCS Á.*

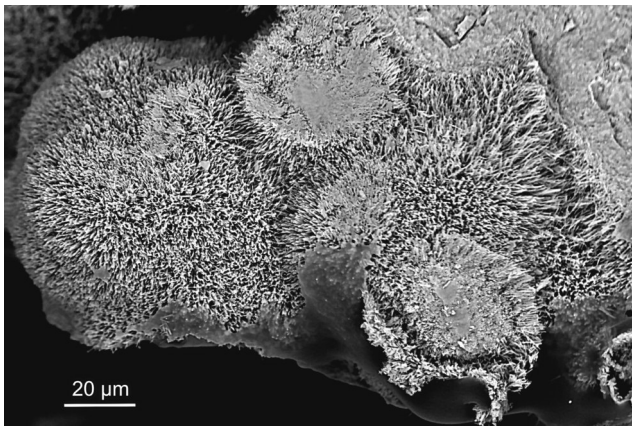

Figure 9. Acicular aggregates of cryptomelane from Buceava-Şoimuş. BSE image. Photo courtesy of Á. KOVÁCS

9. ábra. *A solymosbucsai kriptomelán tűs halmazai. Visszaszórtelektron-kép. Fotó: KOVÁCS Á.*

Table VIII. Electron-microprobe analyses of braunite from Buceava-Şoimuş, Romania, in wt%

VIII. táblázat. *A solymosbucsai (Románia) braunit elektronmikroszondás elemzései tömegszázalékban*

	(1)	(2)	(3)	(4)	(5)
SiO_2	10.04	10.09	10.21	10.08	10.27
Al_2O_3	0.42	1.76	0.35	0.44	0.31
Mn_2O_3*	73.09	76.00	72.77	76.48	72.46
Fe_2O_3**	4.53	0.47	5.92	1.36	5.92
CaO	2.17	1.78	1.54	1.99	1.76
MnO*	8.70	9.70	9.40	8.90	9.00
Total	**98.95**	**99.80**	**100.19**	**99.25**	**99.72**
Cation numbers based on 12 oxygens Kationszámok 12 oxigénre					
Si	1.01	1.00	1.02	1.01	1.03
Σ*T*	**1.01**	**1.00**	**1.02**	**1.01**	**1.03**
Al	0.05	0.21	0.04	0.05	0.04
Mn^{3+}	5.61	5.75	5.52	5.85	5.51
Fe^{3+}	0.34	0.04	0.44	0.10	0.45
Σ*B*	**6.00**	**6.00**	**6.00**	**6.00**	**6.00**
Ca	0.23	0.19	0.16	0.21	0.19
Mn^{2+}	0.74	0.82	0.79	0.76	0.76
Σ*A*	**0.97**	**1.01**	**0.95**	**0.97**	**0.95**

Other measured, but undetected elements: Ti, Cr, Ni, Mg, Na and K. / *Egyéb mért, de nem detektált elemek: Ti, Cr, Ni, Mg, Na és K.*

* Total manganese was measured as Mn_2O_3. Mn^{3+}/Mn^{2+} ratio was calculated from the stoichiometry, i.e. Al + Mn^{3+} + Fe^{3+} = 6 apfu. / *Összes mangán Mn_2O_3-ként mérve. Az Mn^{3+}/Mn^{2+} arány a sztöchiometrikus összetételből számolva, azaz Al + Mn^{3+} + Fe^{3+} = 6 apfu.*

** Total iron was measured as Fe_2O_3. / *Összes vas Fe_2O_3-ként mérve.*

Ukraine

Evenkite-like material from Beskids railway tunnel, Oporets, Eastern Beskids

The characteristic formations of the Cretaceous–Paleogene flysch zone of the Ukrainian Carpathians are a few cm, exceptionally 10–20 cm thick veins formed from deep karst solutions, consisting of calcite, in which well-developed, euhedral quartz crystals are known ("Marmarosh diamond" variety) (LAZARENKO et al. 1963). The quartz often contains hydrocarbon inclusions, giving the crystals a brownish colour and a yellow fluorescence under UV light. In their surroundings, black asphaltene-like material consisting of a mixture of hydrocarbons, classified as pyrobitumen, were described as "elkerite" by LAZARENKO et al. (1963). In 2016, sandstone excavations of a new railway tunnel near the village of Oporets revealed a lot of calcite veins with "Marmarosh diamonds". Rarely, pale yellow, soft aggregates resembling candle wax was observed on calcite in the cracks. This wax is a paraffin, precipitated from migrating hydrocarbons. This phenomenon is well known and studied in detail in oil well tubes (see e.g., HUNT 1962).

The low temperature normal paraffins have an ideal formula of C_nH_{2n+2}, and they crystallize in three groups: the

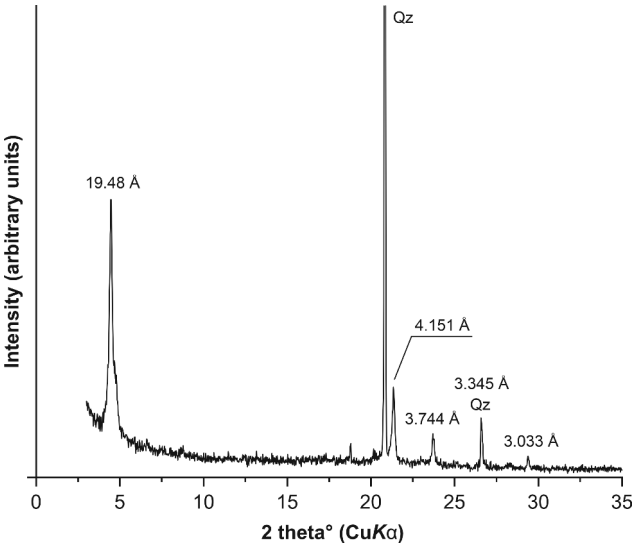

Figure 10. X-ray powder diffraction pattern of evenkite-like material from Oporets
10. ábra. *Az oporeci evenkitszerű anyag röntgen-pordiffrakciós felvétele*

structure is triclinic when n even and n = 6–26, orthorhombic when n odd and n = 11–39, and monoclinic when n even and n = 28–36 (HEYDING et al. 1990). Currently, only one paraffin compound is known as a mineral species, namely evenkite. It was described back in 1953 (SKROPYSHEV 1953),

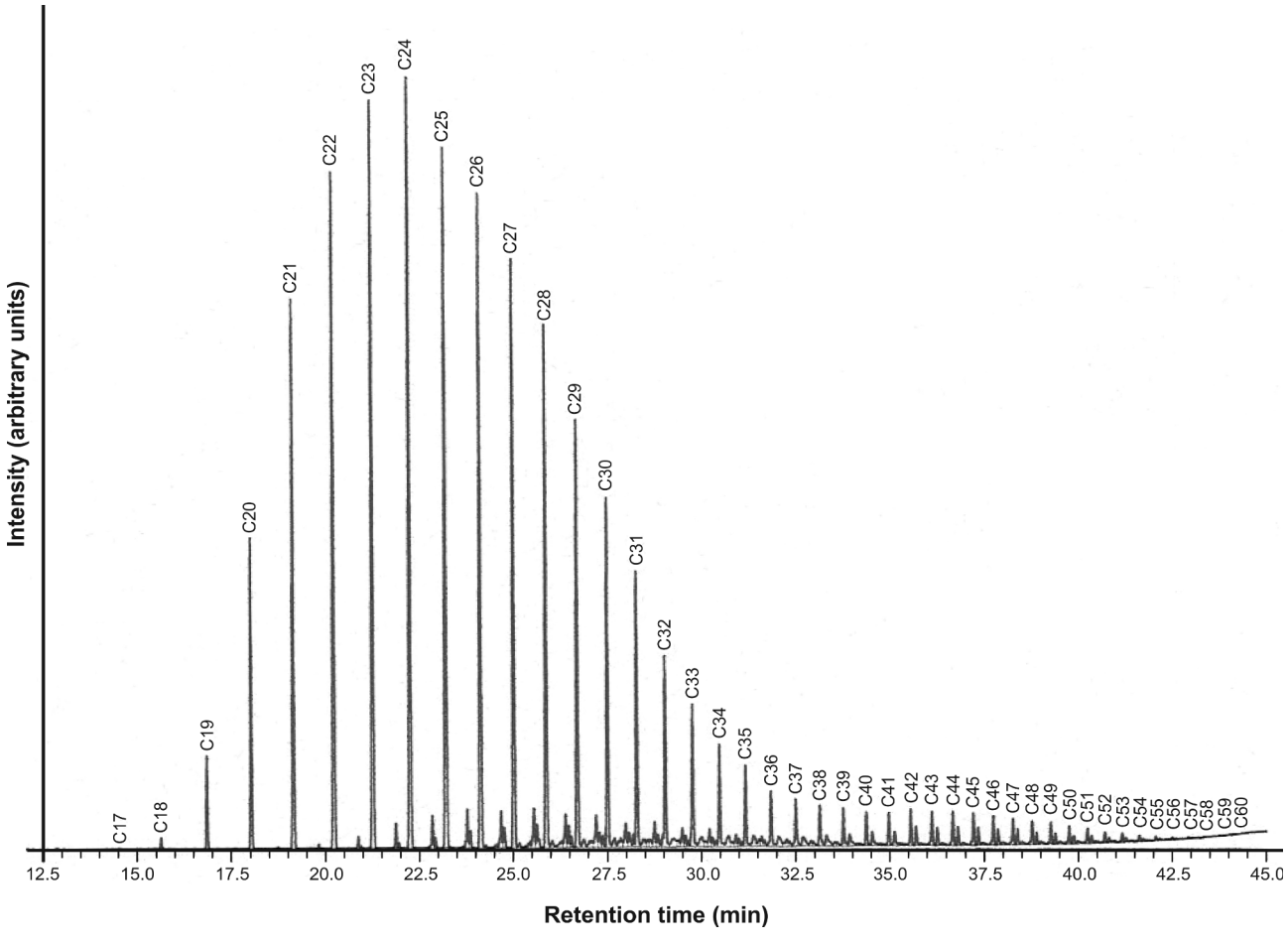

Figure 11. Gas chromatogram of evenkite-like material from Oporets
11. ábra. *Az oporeci evenkitszerű anyag gázkromatográfiás felvétele*

and is listed with grandfathered (G) status by the International Mineralogical Association (IMA 2025). Evenkite is a rather unstable mineral. At room temperature it is a crystalline orthorhombic phase with composition of $C_{23}H_{48}$. However, above 26.3 °C evenkite transforms into various rotational crystalline phases and then melts at 48.8 °C (KOTEL'NIKOVA et al. 2004).

The determination of Oporets paraffin was carried out by X-ray powder diffraction and gas chromatography. On the XRPD pattern (*Figure 10*) only five reflections can be attributed to the paraffin; according to HEYDING et al. (1990), it could be an orthorhombic modification, like evenkite. The detected peaks show good agreement with the data of the ICDD 00-028-2004 card (evenkite), except that the reflection around 19.5 Å was not listed in the latter.

Gas chromatography (GC) results (*Figure 11*) show that the specimens are mixtures of n-paraffins in the range of C17 to C60 with C24 being the most abundant component. Isoparaffins are also detectable on the chromatogram.

Based on the studies presented above, it can be concluded that the Oporets paraffin is an evenkite-like material, which probably has a rich thermal history. For this reason, a wide range of normal paraffins and isoparaffins can be found in it, similar to other evenkite occurrences in the world. Can we consider such a mixture as a mineral? It would be useful to reconsider the mineral status of the evenkite in the future and, if necessary, to develop an appropriate nomenclature for natural paraffins.

Acknowledgements

We thank the help of Bálint PÉTERDI (SARA, Budapest) for selecting suitable braunite samples for the investigations. Many thanks for János BORSODY (Budapest), who provided us with many mineral samples from the Oporets railway tunnel. The first chamosite samples from Egerbakta were submitted for testing by Sándor HOLLÓ (Bükk National Park Directorate, Eger). István SAJÓ (University of Pécs, Pécs) is thanked for the XRPD measurement, and László SZABÓ (Debrecen) for gas chromatography investigation of evenkite. We also thank the two reviewers, Csanád LÓRÁNTH (Lóránth Kőbánya Kft.) and Péter RÓZSA (University of Debrecen) for improvements and comments on the manuscript.

We dedicate this paper to the memory of our good friend and colleague, the late Árpád Kovács (1958–2025).

References

AKASAKA, M., KIMURA, Y., OMORI, Y., SAKAKIBARA, M., SHINNO, I. & TOGARI, K. 1997: ^{57}Fe Mössbauer study of pumpellyite-okhotskite-julgoldite series minerals. – *Mineralogy and Petrology* **61**, 181–198. https://doi.org/10.1007/BF01172483

B. KISS, G., MOLNÁR, F. & PALINKAŠ, L. A. 2016: Hydrothermal processes related to some Triassic and Jurassic submarine basaltic complexes in northeastern Hungary, the Dinarides and Hellenides. – *Geologia Croatica* **69/1**, 39–64. https://doi.org/10.4154/gc.2016.04

B. KISS, G., OELBERG-PÁNCZÉL, E., JANKA, P., KÁPOSZTÁS, V., SZÜCS, L., REASCOS, H., SZABÓ, D., KOVÁCS, D., LIPP, K., SZENDREI, Zs. & NÉMETH, T. 2024: Complex geological study of the quartz vein of the Ősi Hill, Pákozd. – *Földtani Közlöny* **154/3**, 299–306 (in Hungarian with English abstract). https://doi.org/10.23928/foldt.kozl.2024.154.3.299

DE GRAVE, E., VANDENBRUWAENE, J. & VAN BOCKSTAEL, M. 1987: ^{57}Fe Mössbauer spectroscopic analysis of chlorite. – *Physics and Chemistry of Minerals* **15**, 173–180. https://doi.org/10.1007/BF00308781

FEHÉR, B., SZAKÁLL, S. & BIGI, S. 2010: Ni-rich mcguinnessite from Eibenthal, Romania: an intermediate phase toward a new hypothetical rosasite-group end-member. – *Acta Mineralogica-Petrographica, Abstract Series* **6**, 495.

FÖLDESSY, J. 1975: Petrological study of a diabase-spilite magmatitic suite, Darnó-hegy (Sirok, Hungary). – 10th CBGA Congress, Bratislava, 55–70.

HEYDING, R. D., RUSSELL, K. E., VARTY, T. L. & ST-CYR, D. 1990: The normal paraffins revisited. – *Powder Diffraction* **5**, 93–100. https://doi.org/10.1017/S0885715600015414

HOLLAND, T. J. B. & REDFERN, S. A. T. 1997: Unit cell refinement from powder diffraction data: The use of regression diagnostics. – *Mineralogical Magazine* **61**, 65–77. https://doi.org/10.1180/minmag.1997.061.404.07

HUNT, E. B. Jr. 1962: Laboratory study of paraffin deposition. – *Journal of Petroleum Technology* **14**, 1259–1269. https://doi.org/10.2118/279-PA

IMA 2025: *The new IMA list of minerals*. – Updated: May 2025. Downloaded from https://cnmnc.units.it/ on May 10, 2025

JÓZSA, S. 1999: *Petrological and geochemical analysis of the submarine igneous rocks of the Darnó Hill [A Darnó-hegyi óceánaljzati magmás kőzetek petrológiai-geokémiai vizsgálata].* – PhD Thesis, Eötvös Loránd University, Budapest (in Hungarian with English abstract).

KOTEL'NIKOVA, E. N., FILATOV, S. K. & CHUKANOV, N. V. 2004: Evenkite: symmetry, chemical composition, identification and thermal behavior. – *Zapiski Vserossiyskogo Mineralogicheskogo Obshchestva* **133/3**, 80–92 (in Russian with English abstract).

Lazarenko, E. K., Lazarenko, E. A., Barishnikov, E. K. & Maligina, O. A. 1963: *Mineralogy of the Trans-Carpathians [Mineralogiya Zakarpat'ya].* – Izdatelstvo Lvovs'kogo Universiteta, Lvov, 614 p. (in Russian).

Nagashima, M., Ishida, T. & Akasaka, M. 2006: Distribution of Fe among octahedral sites and its effect on the crystal structure of pumpellyite. – *Physics and Chemistry of Minerals* **33**, 178–191. https://doi.org/10.1007/s00269-006-0066-1

Nagy, L. 1958: *Geology of the People's Republic of Romania, Vol. I. [A Román Népköztársaság földtana. I. kötet].* – Bolyai Tudomány-egyetem, Kolozsvár, 770 p. (in Hungarian).

Németh, N., Szakáll, S. & Kristály, F. *in prep.*: Braunite-dominated manganese mineralization in the Telekes Valley, Rudabánya Mts., N-Hungary.

Savul, M. 1932: Note sur la présence du nickel dans les serpentines chromifères du Banat. – *Buletinul Societății Române de Geologie* **1**, 16–17.

Skropyshev, A. V. 1953: A paraffin in a polymetallic vein. – *Doklady Akademii Nauk SSSR* **88/4**, 717–719 (in Russian).

Strusievicz, O. R. 1995: Mineralogical composition of the "green crusts" in the podiform chromites of the Tisovița-Iuți ophiolites (Southern Banat, Romania). – *Romanian Journal of Mineralogy* **76/2**, 91–93.

Udubașa, G., Edelstein, O., Pop, N., Istrate, G., Kovács, M., István, D., Bogancsik, V. & Roman, L. 1982: Magnesian skarns from Țibleş: preliminary data. – *Dări de Seamă ale Şedințelor* **66/2** (1979), 139–156.

Manuscript received: 19/06/2025